LIMNOLOGY and OCEANOGRAPHY



© 2024 The Authors. *Limnology and Oceanography* published by Wiley Periodicals LLC on behalf of Association for the Sciences of Limnology and Oceanography. doi: 10.1002/lno.12525

Rubisco in high Arctic tidewater glacier-marine systems: A new window into phytoplankton dynamics

Megan E. Roberts ¹ Maya P. Bhatia ¹, ², [†] Elden Rowland ¹, Patrick L. White ¹, ² Stephanie Waterman ¹, Maria A. Cavaco ¹, Patrick Williams ¹, Jodi N. Young ¹, Jenifer S. Spence ¹, Jean-Éric Tremblay ¹, Patrick Williams ¹, Patrick L. White ¹, Patrick L. Whi

Abstract

The hundreds of tidewater glaciers found in the Canadian Arctic Archipelago have the potential to enhance delivery of nutrients and other material to the surface ocean. Despite this, their influence on marine ecosystems, specifically phytoplankton, is poorly characterized. Here we developed and applied a quantitative mass spectrometry-based approach to measure phytoplankton ribulose-1,5-bisphosphate carboxylase/oxygenase (Rubisco) concentrations to examine differences in productivity in glacierized and non-glacierized marine systems in Jones Sound, Nunavut, within Inuit Nunangat. Comparisons to chloroplast 16S rRNA gene amplicon sequencing data suggested that these measurements detect the majority of Rubisco produced in Jones Sound. Because Rubisco catalyzes carbon fixation, we used these measurements to estimate total and group-specific primary production potential, which were within the range of historical primary production measurements made using classical methods in this region. Our measurements also revealed that up to 2% of total protein in the water column is Rubisco, and that Rubisco concentrations are correlated with chlorophyll fluorescence, with maxima near the nitracline. Rubisco produced by diatom genera Chaetoceros and Thalassiosira were higher in marine regions influenced by glaciers, while Rubisco from Micromonas (Chlorophyta) was greater in non-glacierized regions. This suggests that future climate scenarios may favor smaller phytoplankton groups, like Micromonas, with consequences for food webs and carbon cycling. This study broadens our understanding of how tidewater glaciers will impact phytoplankton communities, now and in a warmer future, and lays the foundation for using this mass spectrometry-based approach to quantify phytoplankton group-specific carbon fixation potential in other marine regions.

*Correspondence: erin.bertrand@dal.ca

This is an open access article under the terms of the Creative Commons Attribution-NonCommercial License, which permits use, distribution and reproduction in any medium, provided the original work is properly cited and is not used for commercial purposes.

Additional Supporting Information may be found in the online version of this article.

Author Contribution Statement: M.E.R. acquired field data, performed protein laboratory work, analyzed data, and wrote the paper with guidance from E.M.B. and M.P.B. M.P.B conceived the research program, acquired field data, assisted in data analysis, and drafted the manuscript. E.R. designed and conducted the mass spectrometry analysis. P.L.W. analyzed molecular sequencing data. S.W. conceived the research program

and analyzed CTD data. M.A.C. performed DNA extractions, built sequencing libraries, and conducted bioinformatic analyses. P.W. assisted in sample collection and CTD data analysis. J.S.S. assisted in bioinformatic and sequencing data analyses. J.N.Y. conducted the meta-analysis shown in Fig. 2 and assisted with data interpretation. J.-E.T. contributed the nutrient measurements from the CCGS Amundsen. J.-C.M.-S. facilitated sample collection aboard the CCGS Amundsen. E.M.B. conceived the research program and this study, acquired field data, directed the method development and data analysis, and drafted the manuscript. All authors contributed to editing and approval of the final version of the manuscript.

[†]Deceased. We tragically lost Dr. Maya Bhatia while this manuscript was in revision. Without her vision and leadership, this work would never have been accomplished. We aim to share and continue this work in her memory and in her honour.

¹Department of Biology, Dalhousie University, Halifax, Nova Scotia, Canada

²Department of Earth and Atmospheric Sciences, University of Alberta, Edmonton, Alberta, Canada

³Department of Earth, Ocean and Atmospheric Sciences, University of British Columbia, Vancouver, British Columbia, Canada

⁴School of Oceanography, University of Washington, Seattle, Washington, USA

⁵Department of Biology, Québec-Océan and Takuvik, Université Laval, Québec, Quebec, Canada

⁶Institut des Sciences de la Mer, Université du Québec à Rimouski, Rimouski, Quebec, Canada

In high-latitude regions, ice masses whose outlet glaciers terminate in the ocean (tidewater glaciers) are releasing increasing amounts of meltwater runoff into the downstream marine environment. The subsequent interaction of this runoff with the coastal marine environment has the potential to significantly impact marine primary production (Hopwood et al. 2020). The delivery of dissolved freshwater-sourced and marine-sourced chemical species (i.e., nutrients and metals) to the surface ocean via the buoyant glacial meltwater plume and its entrainment of deep seawater has been found to enhance primary productivity in many high-latitude regions (Meire et al. 2017). This is in part due to the timing of the melt, which largely comes at the height of summer when surface nutrient concentrations are drawn down after the spring bloom (Tremblay et al. 2015), but when light availability is still high. Simultaneously, the sediment load delivered with glacial meltwater runoff can increase light attenuation, thereby causing light limitation of phytoplankton growth (Murray et al. 2015).

Across the Arctic, nitrate delivery by tidewater glacial marine systems has been tied to higher primary production using in situ chlorophyll a (Chl a) measurements, carbon fixation rate estimates, and remote sensing analyses (Meire et al. 2017; Vonnahme et al. 2021; Dunse et al. 2022), but there have been very few studies evaluating the impact of tidewater glaciers on marine phytoplankton community dynamics (Kanna et al. 2022; Maselli et al. 2023). Despite the high density of tidewater glaciers across Nunavut in the Canadian Arctic Archipelago, there have been no comprehensive studies investigating interactions between phytoplankton and glaciers in this region. Jones Sound is a marine waterway located in Inuit Nunangat, south of Ellesmere Island and north of Devon Island in Nunavut, and is home to the Inuit hamlet of Ausuittug (Grise Fiord), the northernmost community in Canada (Fig. 1). Residents of this community rely on this marine region for subsistence hunting (Audlaluk 2020) and have observed increased productivity at the termini of glaciers (J. Qaapik, Grise Fiord Rangers, pers. comm.). Some initial, pioneering work in this region during the spring in the 1960s found higher macronutrient concentrations in a fiord with a tidewater glacier relative to one without (Apollonio 1973). Nearly 60 years later, a study conducted in the summer drew similar conclusions and found that surface waters surrounding tidewater glaciers had significantly higher concentrations of macronutrients and micronutrients compared areas without tidewater glaciers, but the impact on phytoplankton communities remains unclear (Bhatia et al. 2021).

Previous studies of phytoplankton within Inuit Nunangat in the Canadian Arctic Archipelago have identified contributions from diverse phytoplankton groups. *Micromonas* spp. appear to be ubiquitously present and important across most of the Arctic under a range of environmental conditions (Monier et al. 2015; Kalenitchenko et al. 2019). During bloom periods, diatoms such as *Chaetoceros, Thalassiosira* and *Fragilariopsis* spp.

tend to dominate (Booth et al. 2002; Kalenitchenko et al. 2019), while dinoflagellates and haptophytes, especially *Phaeocystis* spp., are commonly present during or after bloom periods (Kalenitchenko et al. 2019).

Studies examining phytoplankton community composition are often paired with primary production (14C, 13C-based), Chl a, and particulate organic carbon measurements, in part to gain an understanding of the contribution of different taxonomic groups to primary production. However, the pairing of these data types for this purpose falls short because neither cell counts nor rRNA gene amplicons have any direct relationship with primary production. To fill this gap, we propose that measurements of the enzyme Rubisco may be useful. Rubisco is the enzyme that catalyzes fixation of atmospheric CO2 and is therefore directly involved in primary production. Rubisco enzymes found in most eukaryotic phytoplankton (Form 1) are composed of eight large subunits (ribulose-1,5-bisphosphate carboxylase/oxygenase [RbcL]) and eight small subunits (RbcS) (Hartman and Harpel 1994), forming four dimers each with two active sites (Tabita et al. 2008). An exception is peridinincontaining dinoflagellates, which possess Form II Rubisco (Morse et al. 1995). Rubisco is inefficient because (1) its carboxylation rate is slow, (2) it is competitively inhibited by oxygen, and (3) it is a large enzyme requiring many accessory proteins to assemble and activate (Lorimer and Andrews 1973). To account for this inefficiency, Rubisco is abundant in marine phytoplankton (Losh et al. 2013; Young et al. 2015a), thereby making it an accessible target to quantify in mixed microbial communities. In addition, Rubisco protein concentrations in marine phytoplankton appear to be highly correlated with carbon fixation rates (Losh et al. 2013), suggesting that measuring this protein in mixed communities may be informative.

Surveys of Rubisco-encoding genes and their expression have been made previously in the ocean: quantitative polymerase chain reaction assays have been used to measure RbcL gene abundance (Pujari et al. 2019) and gene expression (John et al. 2007) from different phytoplankton taxa. Quantitative western blots have been used to obtain measurements of Rubisco as a percentage of the total protein in communities (Losh et al. 2013; Young et al. 2015a,b). Previous measurements of Rubisco enzyme activity and Chl a patterns have also been made in Jones Sound, revealing that Rubisco activity was highly correlated with Chl a concentration and distributed in similar patterns throughout the mixed layer of the water column (Harrison et al. 1987). However, these past analyses of Rubisco activity in marine phytoplankton have not provided absolute quantification of the protein, nor have they been able to resolve which phytoplankton groups are responsible for Rubisco production.

In this study, we apply a mass spectrometry-based technique to measure the concentration of the RbcL at a variety of sites with varying tidewater glacier influence in Jones Sound. We assessed the proportion of the phytoplankton community

Roberts et al. Rubisco in glacier-marine systems

that is targeted by these RbcL measurements, and then applied them to determine how Rubisco concentrations are impacted both by (1) biogeochemical variables down the water column and (2) marine environments with varying glacier meltwater input throughout Jones Sound. We also use these measurements to estimate maximum potential carbon fixation rates and apportion that carbon fixation potential to key phytoplankton groups. Determining which groups of phytoplankton contribute to carbon fixation and how they respond to melting glaciers is critical to enhancing our understanding of potential changes to marine biogeochemical cycles and Arctic food webs into the warming future (Miller and Wheeler 2012).

Methods

Study site

Jones Sound is a waterway north of Devon and south of Ellesmere Islands. Water flows into Jones Sound from Nares Strait to the east and Hell Gate to the west; currents generally flow west along the north side of the sound and east along the south side, exiting into Baffin Bay (Jones et al. 2003; Fig. 1, arrows). There are numerous tidewater glaciers that drain into Jones Sound. In this study, we conducted near-terminus (< 25 km) sampling of the ocean at Sydkap and Jakeman Glaciers on Ellesmere Island, as well as Sverdrup and Belcher

Glaciers on Devon Island (Fig. 1). During summer months (July–August) surface nutrient concentrations are elevated in the marine region proximal to these glaciers as a result of upwelling of deep seawater (Bhatia et al. 2021). These four glacier systems are thought to fall along a continuum of increasing influence on the marine environment from Belcher Glacier as a strongly tidewater glacier influenced system to Jakeman Glacier as a weakly tidewater glacier influenced system with Sydkap and Sverdrup Glaciers falling in between (Bhatia et al. 2021). Two nearshore non-glacierized sites were also sampled: Grise Fiord on Ellesmere Island and a site near Truelove Inlet on Devon Island (Fig. 1). In addition to these nearshore sites, offshore sampling occurred across open Jones Sound, the eastern gateway and just outside of the sound on the western edges of Baffin Bay (Fig. 1).

Sample collection

Samples were collected in late summer of 2019 during two expeditions: on the *CCGS Amundsen* from 06 August to 10 August and on the *S/Y Vagabond* from 22 July to 16 August. Coordinates and sampling details for all sampling stations are outlined in Supporting Information Table S1.

On the *CCGS Amundsen*, vertical profiles of in situ measurements of water column properties were collected using a conductivity, temperature, and depth (CTD) profiler (SBE-911plus, Sea-Bird Electronics Inc.) with additional sensors for chlorophyll

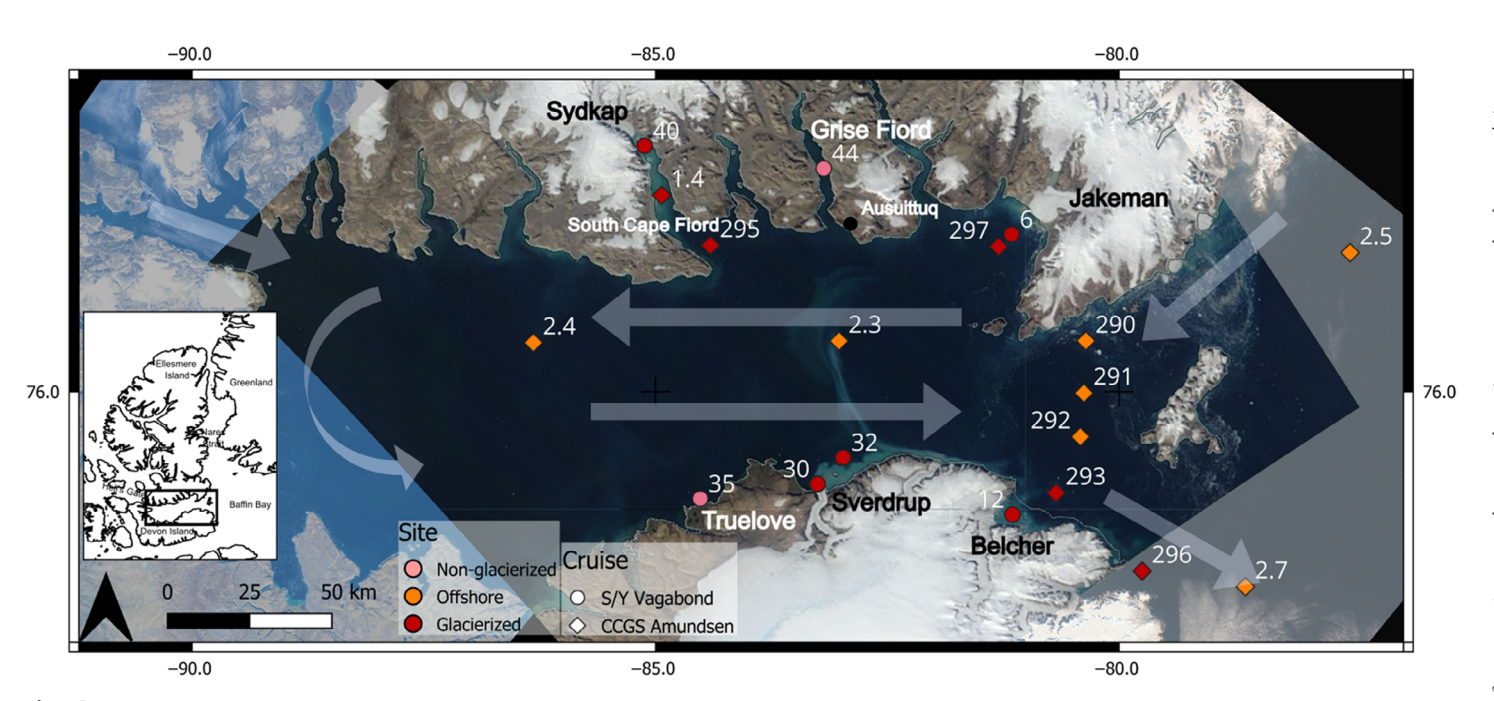


Fig. 1. Map of the study area in Jones Sound, NU in Inuit Nunangat. Locations of sampling stations are labeled with station numbers and indicated by colored symbols: diamonds indicate stations sampled during Leg 2b of the *CCGS Amundsen* 2019 summer cruise and circles indicate the stations sampled from the *S/Y Vagabond*, also in summer 2019; stations colored red are considered glacierized sites (< 25 km from tidewater glacier), stations colored pink are considered nearshore non-glacierized sites (< 20 km from shore, but > 25 from any tidewater glacier), and stations colored orange are classed as offshore sites (> 20 km from shore). Arrows on map indicate dominant surface current direction (see Jones et al. 2003). The six distinct nearshore study sites are indicated (four glacierized sites: Jakeman, Belcher, Sverdrup, and Sydkap Glaciers; two non-glacierized sites: Grise Fiord and Truelove Inlet). Base images: Landsat 8 OLI/TIRS C1 Level 1, August 2019, US Geological Survey and National Aeronautics and Space Administration.

fluorescence (SCF, Seapoint), light intensity (photosynthetically active radiation [PAR]—QCP 2300, Biospherical Instruments), and dissolved oxygen (SBE 43, Sea-Bird Electronics Inc.). Seawater samples were also collected in 12-liter Niskin bottles on a rosette. For protein samples, water was collected from the Niskin bottles into acid-clean 10-liter high density polyethylene (HDPE) carboys and filtered sequentially through 3.0- and 0.2-µm poresize polycarbonate filter membranes using a peristaltic pump, tygon, and silicon tubing. Collection was complete within 3 h of the rosette's recovery. Filters were then stored in 2-mL cryovials and frozen in a -80°C freezer. Protein samples were collected from four depths at each station, typically near surface (2 m depth), the depth of the subsurface chlorophyll maximum (SCM), the depth of a second deep chlorophyll max (if present), and at a depth at least 100 m below any detectable fluorescence signal from the sensors. Nutrients were sampled directly from the Niskin bottles through a glass fiber filter (GF/F, Whatman) into acid-cleaned polyethylene tubes and stored in the dark at 4°C. Concentrations of nitrate + nitrite, nitrite, phosphate, and silicate were measured calorimetrically (Hansen and Koroleff 1999) with a Bran and Luebbe AutoAnalyzer III within a few hours of collection onboard. Analytical detection limits were $0.03 \,\mu\text{M}$ for nitrate, $0.02 \,\mu\text{M}$ for nitrite, $0.05 \,\mu\text{M}$ for phosphate, and 0.1 μ M for silicate. Nutrient samples were collected at 12–20 depths per station. Sampling from CCGS Amundsen included glacierized stations (< 25 km from tidewater glaciers) and offshore stations (> 25 km from shore). This categorization of sites is intended to summarize broad patterns and does not necessarily reflect the full range of local processes that may influence phytoplankton dynamics.

On the S/Y Vagabond, vertical profiles of water column properties were measured using a fast (8 Hz) profiling multichannel logger (RBR Ltd/RBRmaestro³) equipped with sensors for conductivity, temperature, pressure, dissolved oxygen (RBRcoda), PAR (Licor Quantum 192SA), Chl a (Turner Cyclops), and turbidity (Seapoint). Seawater samples for nutrient, protein, and DNA analyses were collected using 10-liter Go-Flo bottles at the SCM depth. For DNA and protein analyses, water was transferred from the Go-Flo bottles into 4-liter polycarbonate bottles at one depth per station (at the chlorophyll maximum) and then filtered through a 0.22-µm SterivexTM filter unit via peristaltic pumping. One liter of water was filtered for DNA sampling and between 2 and 5 liters of water was filtered for protein sampling. Residual water was pushed through the SterivexTM with a clean syringe before the filter was capped, flash frozen, and stored in a dry shipper charged with liquid nitrogen for transport and then transferred to a -80°C freezer. Water for nutrient samples was filtered through a 0.22-µm polyethersulfone syringe filter into acid-clean, 3× samplerinsed 20-mL HDPE plastic scintillation vials and frozen (-20°C) until analysis. Concentrations of nitrate, nitrite, phosphate, and silicate were measured colorimetrically on a Skalar SAN++ Continuous Flow Nutrient Analyzer within 1 month of collection at the Dalhousie CERC.OCEAN Laboratory as per McGrath et al. 2019. Analytical detection limits were $0.05 \mu M$ for nitrate, $0.01 \mu M$ for nitrite, $0.01 \mu M$ for phosphate, and $0.05 \mu M$ for silicate. Sampling from the Vagabond included sites that were glacierized (< 25 km from a tidewater glacier), offshore (> 25 km from shore), and non-glacierized (> 25 km from a tidewater glacier and < 25 km from shore).

Euphotic zone depth was calculated as the depth where PAR = 0.1% of the surface value, as in (Banse 2004) and nitracline depth was defined as where change in $[NO_3^-]$ /change in Z is greatest.

RbcL sequence database

To select appropriate RbcL peptide sequences for this study, a database of RbcL protein sequences from phytoplankton was compiled. Protein sequences (FASTA) similar to Type I RbcL from *Emiliania huxleyi* (Tabita et al. 2007, 2008) were retrieved using the protein BLAST as described in the Supporting Information. In total, there were 423 RbcL sequences in the resulting database, a subset of which are shown in Fig. S1.

Peptide selection

To measure Rubisco concentration from important phytoplankton groups, peptides that were conserved across relevant taxonomic groups for our study area were chosen a priori. At the time of peptide selection, DNA and RNA sequence data from the sites sampled for protein analysis was not yet available. Therefore, we based Rubisco peptide decisions on the available literature of the phytoplankton community composition across the region at the time (Lovejoy 2014; Joli et al. 2018; Kalenitchenko et al. 2019). We leveraged our Rubisco database to select sequences from the following phytoplankton groups: diatoms, haptophytes (with a focus on Phaeocystis), and green algae (with a focus on Micromonas spp.). MUSCLE (Madeira et al. 2022) alignments of sequences from each of these groups were prepared and inspected for tryptic peptides conserved within each group. The consensus sequence from each alignment was analyzed using the tool PeptideCutter (Gasteiger et al. 2005) and any potentially useful peptides were checked for taxonomic specificity using Unipept (Gurdeep Singh et al. 2019). The selected peptides are summarized in Supporting Information Fig. S2. Together, the three diatom peptides selected are predicted to be encoded in 86% of the diatom RbcL sequences (n = 91). The haptophyte peptide is encoded in 50% of the 12 Haptophyta sequences, including all available Phaeocystis spp. RbcL sequences (n = 3). The *Micromonas*-specific peptide is encoded in 25% of the available green algal sequences (n = 16), including the available *Micromonas* spp. RbcL sequences (n = 2).

Protein extraction and digestion

Protein was extracted from 0.2- and 3.0- μ m polycarbonate filters and 0.22- μ m SterivexTM filters and digested into tryptic peptides using S-trap columns, following Joy-Warren et al. 2022, as described in the Supporting Information with the following modification: 750 μ L of 2% sodium dodecyl

sulfate (SDS) extraction buffer (0.1 M Tris/HCl pH 7.5, 5% glycerol, 5 mM EDTA, 2% SDS) was added to each sample.

Targeted RbcL measurements

Targeted metaproteomic analysis was performed using an UltiMate 3000 UHPLC (Dionex) coupled with a TSQ Quantiva mass spectrometer (Thermo Scientific) with operations and settings as described by Wu et al. 2019. Samples were diluted with 1% formic acid, 3% acetonitrile to a final peptide concentration of 0.167 μ g μ L⁻¹. Each sample was spiked with either 3.3 or 6.6 fmol μL^{-1} of each heavy isotope-labeled internal standard for each peptide (Thermo Scientific, Supporting Information Table S1). Injections of $6 \mu L$ were performed in triplicate. Selected reaction monitoring (SRM) transitions were optimized on our instrument using the Quantiva Transition Optimization tool. The method contained 86 transitions (Table S2). All raw targeted metaproteomic data obtained from the mass spectrometer were processed using Skyline-daily software (Pino et al. 2017). RbcL peptide concentrations were calculated from the mass spectrometry data by multiplying the peak area of each peptide of interest by the ratio of moles of the heavy isotope-labeled version of that peptide added to the peak area corresponding to that heavy isotope-labeled peptide. For peptides containing the amino acid methionine, which can be oxidized, peak areas of oxidized and non-oxidized forms of the peptide were summed together. Concentrations of each peptide from 3 and 0.2 μ m size fraction filters, if available, were summed.

DNA extraction, sequencing, and computational analyses

DNA was extracted from the 0.2- μ m SterivexTM filters using a phenol chloroform protocol as described in the Supporting Information.

We amplified the V4–V5 hypervariable region using published primer sets (515F, Parada et al. 2016; 926R, Quince et al. 2011) of the 16S rRNA gene for prokaryote composition and the V4 hypervariable region (E572F, E1009, Comeau et al. 2011) of the 18S rRNA gene for eukaryotes as described in the Supporting Information. Amplicons were sequenced on a MiSeq instrument (Illumina Inc. using a 2 \times 250 cycle MiSeq Reagent Kit v3, Illumina Canada Inc.), processed, and clustered into amplicon sequence variants (ASVs) as described in the Supporting Information. 4.4% of ASVs were assigned to chloroplasts making up an average of 12.2% of the total reads in each sample, with the rest being assigned to prokaryotes.

16S chloroplast rRNA gene amplicon sequencing comparison

To compare the RbcL concentration data with 16S chloroplast rRNA gene amplicon sequencing data, we classified the ASVs based on how they relate to the groups that our RbcL peptides target. We conducted two separate analyses, one examining how the 16S rRNA gene amplicon data compared to the groups we expected to target with our broad RbcL peptide, and a second examining how they compared to the taxon-specific RbcL

peptides. For the second analysis, the three diatom peptides were grouped together for simplicity. Any ASVs in the 16S chloroplast data associated with organisms that were not expected to encode any of the RbcL peptides were classified as "other." The remaining ASVs were grouped into one of three groups: diatom, haptophytes, or *Micromonas* spp. Within each of these three groups, there were two distinctions based on the taxonomic resolution each ASV was assigned: (1) ASVs from phytoplankton groups that contain sufficient taxonomic specificity to suggest that their originating organisms would encode the corresponding RbcL peptide and (2) ASVs that were associated with the assigned group but lack taxonomic specificity, making it uncertain that their originating organism would encode the associated RbcL peptide.

Calculations of Rubisco as a percentage of total protein

Form 1 Rubisco contains eight each of large and small subunits (Baker et al. 1975), therefore equimolar stoichiometry can be used in conjunction with the molecular weights of 55 and 15 kDa for RbcL and RbcS, respectively, to make calculations of Rubisco as a % of total protein (Baker et al. 1975). The following equation was used to calculate the % Rubisco of total protein for each peptide in the samples:

$$mol RbcL = mol RbcS$$
 (2)

Mass of RbcL =
$$molof RbcL \times 55,000 (g RbcL/mol)$$
 (3)

Mass of RbcS =
$$mol of RbcS \times 15,000 (g RbcL/mol)$$
 (4)

$$\frac{RbcL\,mass + RbcS\,mass}{total\,sample\,protein\,(g)} \times 100 = \% Rubisco\,of\,total\,protein \quad (5)$$

Estimating maximum potential carbon fixation rates

RbcL concentrations were used to estimate maximum potential carbon fixation rates. Since Rubisco contains eight large subunits and has eight active sites, 1 mol RbcL = 1 mol active site. Assuming CO₂ saturation and all active sites are active, a maximum turnover rate ($k_{\rm cat}^c$) of 0.4 mol C s⁻¹ mol⁻¹ RbcL (*see* Supporting Information and Fig. S3) can be used to estimate the carbon fixation rates as:

Carbon fixation rate
$$\left(\text{mg C m}^{-3} \text{ d}^{-1}\right)$$

= RbcL(mol L⁻¹) × k_{cat}^c (mol C active sites⁻¹ s⁻¹)
× $\frac{1 \text{ mol active site}}{1 \text{ mol RbcL}}$ × 12.011(g C mol⁻¹) × 1000 (L m⁻³)
× 86,400 (s day⁻¹)

While there is variability in maximum turnover rate (k_{cat}^c) amongst organisms at mesophilic temperatures this variability appears to be reduced at low temperatures.

Roberts et al. Rubisco in glacier-marine systems

Results

Introducing and evaluating rubisco peptide measurements

We identified six Rubisco large subunit (RbcL) peptides that target key phytoplankton groups, one with broad taxonomic coverage and five with taxon-specificity, covering three groups of diatoms, *Phaeocystis* and *Micromonas* (Supporting Information Fig. S2).

We found a strong linear correlation between measurements of the broad eukaryotic RbcL peptide (y-axis) and the sum of the group-specific RbcL peptide concentrations (x-axis) (Fig. 2). In a single-organism proteomic study, we generally expect two peptides from the same protein to be present in cells at a relatively constant 1:1 proportion. Similarly, we expect a strong linear relationship between the broad eukaryotic RbcL peptide and the sum of the specific RbcL peptides. With an R^2 value of 0.86, this regression indicates that there is such a relationship between the broad peptide and the sum of individual peptide concentrations. Since the broad eukaryotic RbcL peptide sequence is found across a larger range of phytoplankton than the individual group RbcL peptides measured here, we do not expect a 1:1 ratio. Notably, the sum of the group-specific RbcL peptide concentrations is consistently lower than the broad RbcL peptide, which may be attributable to uncharacterized diversity in RbcL sequences among groups

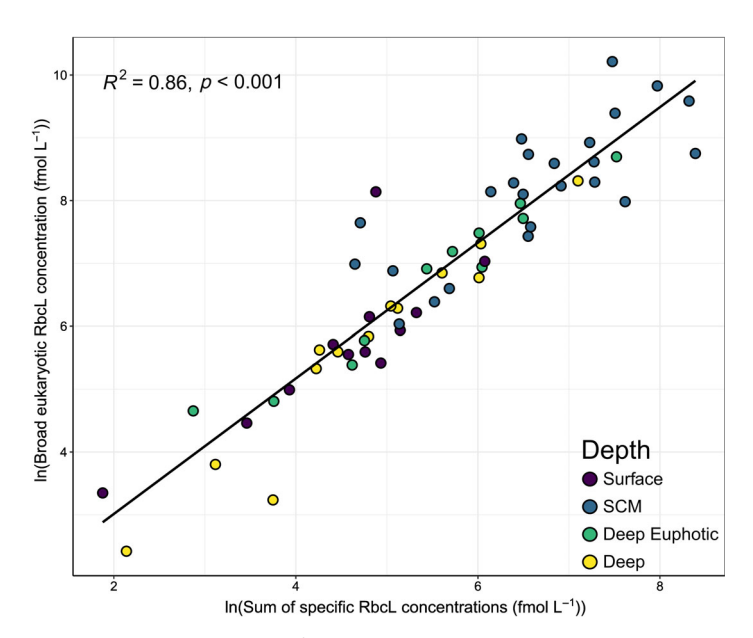


Fig. 2. Linear regression (R^2 and p-value displayed, upper left corner) of the natural logarithm of the sum of the group-specific RbcL peptide concentrations (DYVAEGPQILR for *Phaeocystis*, FLNCMEGINR, FLNCLENGINR, FLYCMEGINR for diatoms) vs. the natural logarithm of the broad eukaryotic Rubisco large subunit (RbcL) peptide (YESGVIPYAK) concentration. *Micromonas* RbcL peptide (NVTLGFVDLMR) concentration is excluded from the sum of individual taxonomic peptides since the broad RbcL peptide is not found within green algae. Samples are colored by depth with SCM indicating subsurface chlorophyll maximum.

targeted by our specific peptides, or contributions from phytoplankton groups that are not targeted with these analyses.

Stacked bars in Fig. 3 display relative proportions of the 16S chloroplast ASVs recovered from six stations sampled on the S/Y Vagabond, classified based on whether the originating organisms are likely to encode RbcL sequences that are detected by either the broad eukaryotic RbcL peptide or the Micromonas RbcL peptide (Fig. 3a), as well as the taxon-specific RbcL peptides (Fig. 3b). These comparisons show that both the broad RbcL peptide, as well as the combination of specific RbcL peptides, are likely to detect a large proportion of the Rubisco produced by these phytoplankton communities. In most cases, ASVs not expected to have RbcL targeted by our peptides made up < 15% of reads with the exception of Sta. 40 in South Cape Fiord (Fig. 5b), where Cryptophytes appear to be significant (Supporting Information Fig. S4). At this site, we estimated that 51% of the reads mapped to ASVs that were associated with organisms with Rubisco sequences that do not include these specific RbcL peptides. However, most of the sequences at this site not captured by the taxon-specific RbcL peptides are covered by the broad eukaryotic RbcL peptide (Fig. 3a). The composition of the "other" section in Fig. 4b for each of these samples is presented in Supporting Information Fig. S4. When we compared the RbcL concentration data, in relative proportion (Fig. 3c), to the 16S chloroplast reads, we found that the average proportion of Haptophyta and diatoms are similar across the two data types: Haptophyta made up $17.1\% \pm 18.4\%$ of the 16S chloroplast data vs. $22.2\% \pm 18.6\%$ of the RbcL data, while diatoms made up $62.5\% \pm 35.2\%$ of the 16S chloroplast data vs. $48.2\% \pm 29.4\%$ of the RbcL data. In contrast, the average proportion of *Micromonas* was higher in the RbcL data relative to the 16S chloroplast data (29.5% \pm 16.9% vs. $5.10\% \pm 7.62\%$). While a similar comparison to 18S rRNA amplicon-based assessments of eukaryotic community composition is not useful because a high proportion of the sequences recovered are from heterotrophic organisms, 18S rRNA gene sequencing confirmed the presence of Micromonas, Phaeocystis, and diatoms (Supporting Information Fig. S7).

Relationships between Rubisco and water column variables

We explored relationships between nutrient concentrations, light, Chlorophyll fluorescence, total protein, and RbcL in the water column at glacierized sites (Fig. 4) and offshore sites (Supporting Information Fig. S5) in order to better understand the contribution of specific phytoplankton groups in this region and their environmental controls. Examining patterns in these depth profile sets across our study region highlighted relationships between RbcL and more traditionally measured biogeochemical parameters. Relationships among nutrient concentrations, light, Chlorophyll fluorescence, total protein, and RbcL throughout the water column are consistent with Rubisco being generated by phytoplankton communities; RbcL maxima are in the euphotic zone, generally coincident with chlorophyll

Rubisco in glacier-marine systems

Roberts et al.

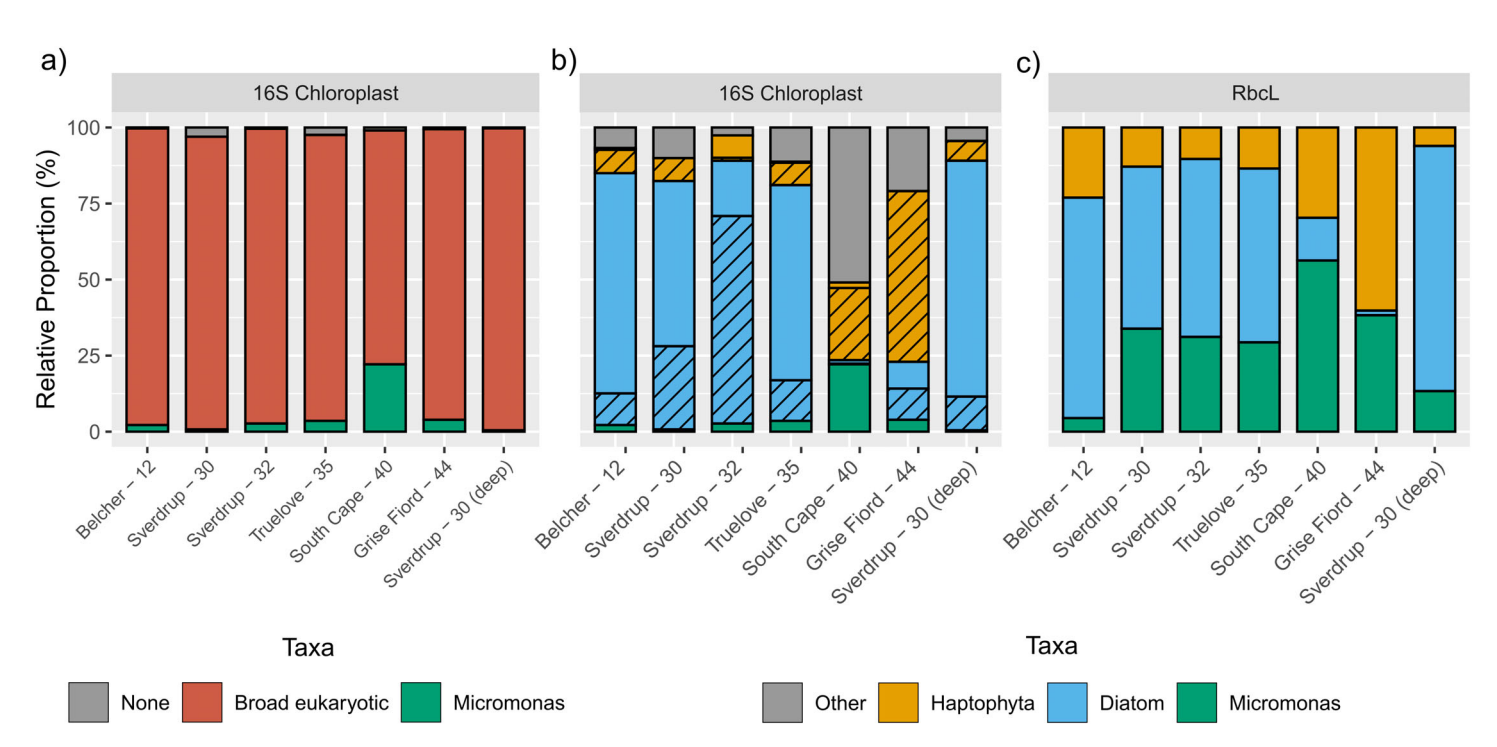


Fig. 3. Comparison of phytoplankton community composition assessed via 16S chloroplast rRNA gene amplicon sequencing (**a,b**) and taxon-specific RbcL quantification (**c**). Unless otherwise noted, these samples were collected aboard the *S/Y Vagabond* at the depth of the subsurface chlorophyll maximum. The "deep" sample was collected at 110 m depth. Stas. 12, 30, 32, and 40 are at glacierized sites, while Stas. 35 and 44 are at non-glacierized sites. (**a**) Assessment of phytoplankton community composition based on the 16S chloroplast sequencing reads; the ASVs are classified according to whether we expect the broad eukaryotic RbcL peptide (red) or *Micromonas* RbcL peptide (green) to be present in Rubisco sequences from the associated organisms. (**b**) Similar assessment based on the same 16S sequencing reads, here classified based on whether we expect the ASVs to be associated with organisms encoding Rubisco sequences with the taxon-specific RbcL peptides. For simplicity, the three diatom peptides are combined. "Other" in panels a and b represents ASVs from phytoplankton groups that we do not expect to produce these RbcL peptides. Hashed bars in (**b**) indicate ASVs that are associated with the assigned group but lack enough taxonomic specificity to be certain that their originating organism would encode the associated RbcL peptide. (**c**) Relative proportion of RbcL ascribed to each phytoplankton group based on peptide measurements.

maxima and in close proximity to the nitracline (with the exception of Fig. 4a and S5e) (Fig. 4; Supporting Information Fig. S5; Tables S6, S7)

RbcL concentrations from diatoms and haptophytes reached maximum values most often at the subsurface chlorophyll maxima depth and near the nutricline (Fig. 4c,e; Supporting Information Fig. S5b-d,g). In contrast, RbcL concentrations from Micromonas spp. were sometimes higher in the water column where there are lower nutrient concentrations (Fig. 4a,d; Supporting Information Fig. S5f). Total protein concentration was also occasionally higher near the surface (i.e., at the first sampling depth, z = 2 m) where nitrate concentration was low and the broad eukaryotic RbcL concentrations remained close to 0 pmol L⁻¹ (Fig. 4b,c,e; Supporting Information Fig. S5b,e). However, the maximum concentrations of both total protein and the broad eukaryotic RbcL peptide usually co-occurred at the subsurface chlorophyll maxima and at, or near, the nitracline with the exception Fig. 4a and Supporting Information Fig. S5e.

A Pearson correlation matrix of the RbcL peptides and total protein concentration compared with other environmental variables (Fig. 5) highlights that each RbcL peptide is

positively correlated with both chlorophyll fluorescence and total protein. This analysis also highlights that *Micromonas* RbcL patterns are distinct from the other target RbcL groups, displaying a stronger relationship with variables that are elevated in the surface, showing significant positive correlations with temperature and PAR, and negative correlations with density, nitrate, and silicate (Fig. 5). In contrast, the Haptophyta, diatom, and broad eukaryotic RbcL peptides showed no significant relationship, or a weaker relationship, with these factors. Scatterplots data used to examine these relationships can be found in Supporting Information Fig. S6.

Regional patterns in Rubisco

The magnitude of Rubisco being produced, as well as the types of phytoplankton producing it, appeared to be influenced by proximity to glacier systems. In general, the average broad eukaryotic RbcL concentration at subsurface chlorophyll maximum depths in the glacierized regions $(8.27 \pm 7.94 \text{ pmol L}^{-1})$ were elevated relative to offshore location $(3.03 \pm 1.82 \text{ pmol L}^{-1})$ (Fig. 6; Supporting Information Table S7), but this difference is not statistically significant

doi/10.1002/lno.12525 by Jodi Young

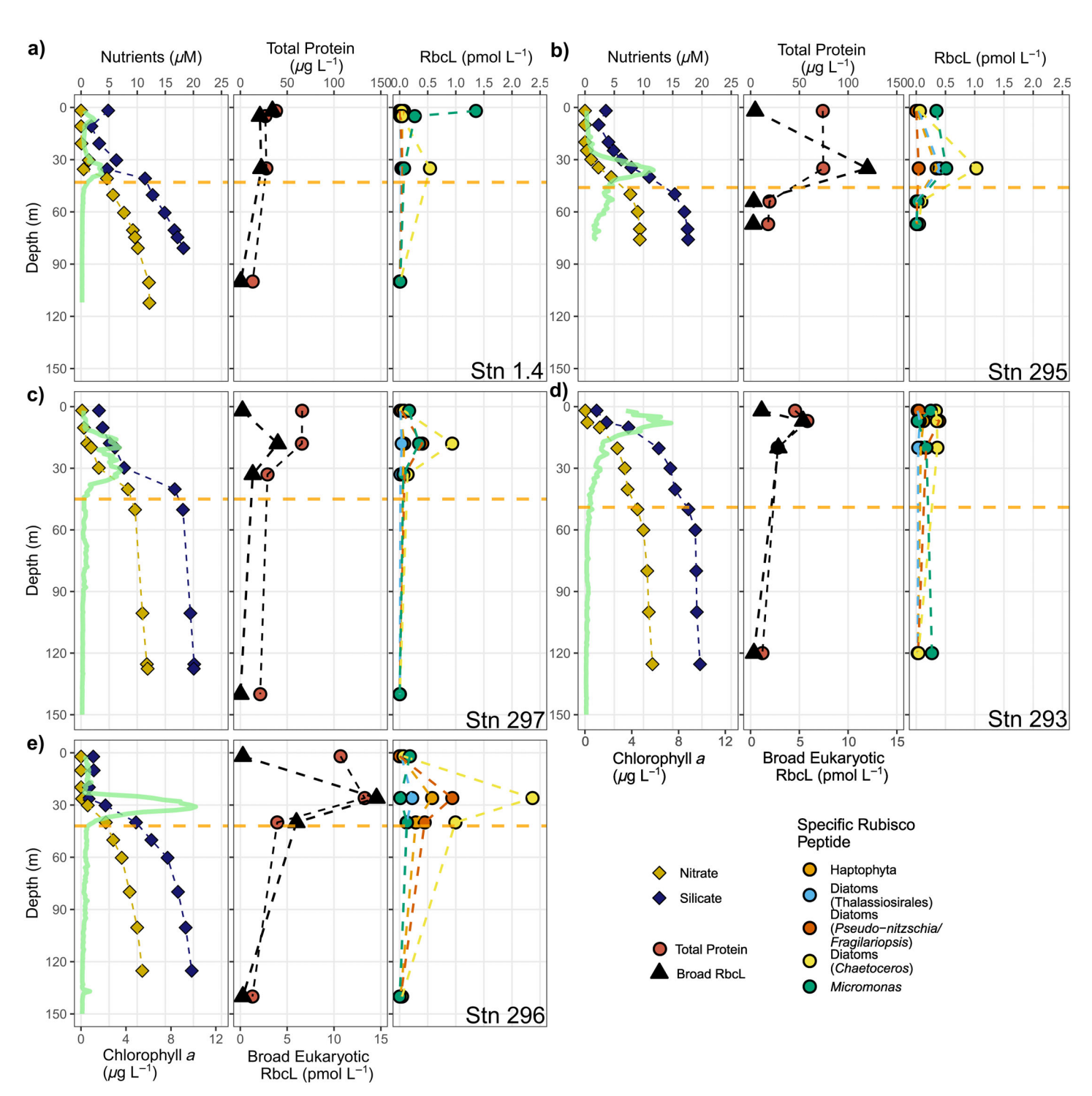


Fig. 4. Depth profiles of sensor-derived in vivo Chl *a* fluorescence (thick light-green line) and bottle measurements of nitrate and silicate concentrations (left), total protein and broad eukaryotic Rubisco large subunit (RbcL) concentration (middle) and RbcL concentrations for five specific phytoplankton groups (right) for glacierized stations (< 25 km from a tidewater glacier) sampled from *CCGS Amundsen*: 1.4 (a), 295 (b), 297 (c), 293 (d), 296 (e). Yellow dotted line across all panels indicates the estimated euphotic zone depth calculated as 0.1% of surface PAR for that station.

(p = 0.07), Wilcoxon rank-sum test). Although broad eukaryotic RbcL concentrations at non-glacierized regions were also elevated relative to offshore locations, the low number of sites classified as non-glacierized disqualifies this category from significance

tests. Examining the partition of RbcL concentrations across the five phytoplankton groups (Supporting Information Table S7) revealed that *Micromonas*, Haptophyta, and the *Pseudo-nitszchia/Fragilariopsis* and *Chaetoceros* diatom groups appear across all

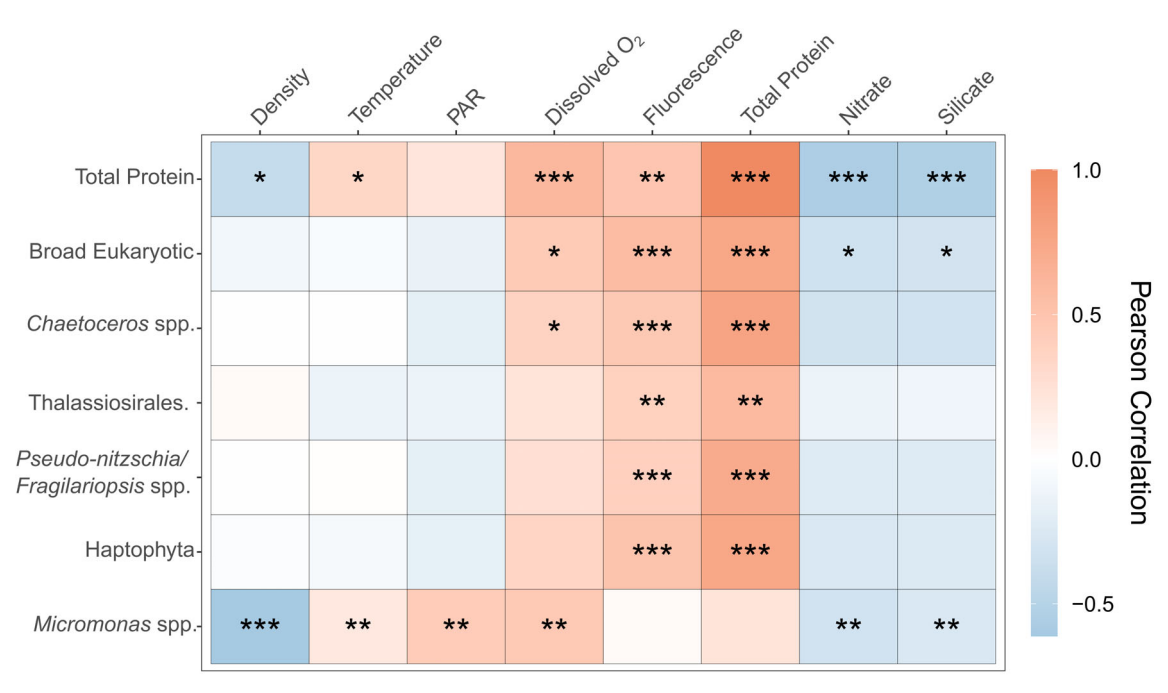


Fig. 5. Correlogram displaying pairwise comparisons of environmental factors with RbcL peptide concentrations and total protein in glacierized (< 20 km from a tidewater glacier) and offshore stations (> 25 km from shore) sampled from *CCGS Amundsen*. Color represents strength/direction of correlation using the Pearson correlation coefficient (r). Red = positive correlation, blue = negative correlation. Asterisks within squares represent the significance level p-value from the correlation coefficient (p < 0.05, **p < 0.01, ***p < 0.001). Blank squares indicate the correlation is insignificant. Water column variables: PAR, Chl p fluorescence (Fluorescence).

three regional categories, while RbcL from the Thalassiosira group is mostly present at glacierized stations only. The principal component analysis in Fig. 6 displays Micromonas and Haptophyta peptides grouped away from the three diatom peptides and generally did not increase concomitantly with the broad RbcL peptide and were most associated with non-glacierized sites. However, trends identified for Micromonas and Haptophyte RbcL appeared to be largely driven by a single station, 44 (Grise Fiord). In contrast, the diatom RbcL peptides and the broad RbcL peptide increase concomitantly (Fig. 6). RbcL concentrations from diatom groups and the broad eukaryotic RbcL peptide were most associated with the glacierized sites, specifically, Chaetoceros RbcL concentrations are significantly higher at glacierized stations $(0.820 \pm 0.630 \text{ pmol L}^{-1})$ compared to offshore stations $(0.339 \pm 0.171 \text{ pmol L}^{-1}) \text{ with } p < 0.05 \text{ (Wilcoxon rank-sum)}$ test) (Supporting Information Table S7). The average RbcL concentration from Thalassiosira in the glacierized category was $0.175 \pm 0.149 \text{ pmol L}^{-1}$, while the average concentration was lower across offshore stations (0.0411 \pm 0.210 pmol L⁻¹) and even lower for non-glacierized stations (0.025 \pm 1.91 pmol L⁻¹).

Estimating potential carbon fixation rates

Converting our Rubisco concentrations into maximum potential carbon fixation rates yields estimates that align with previous primary productivity measurements made in situ in nearby regions (Table 1). The most recently available productivity assessments from Jones Sound were made in the early

1980s using 14 C uptake experiments. These measurements were made during a similar time of year and ranged from 0.001 to 2.016 with an average of 0.43 mg C m $^{-3}$ d $^{-1}$ (Irwin et al. 1985). Using our Rubisco measurements, we predict a range of 0.01–11.7 and an average of 1.25 mg C m $^{-3}$ d $^{-1}$. The range and average values of primary productivity from broader Baffin Bay, collected in the late 1970s using 14 C uptake experiments, are higher than our calculated rates, but still within a similar magnitude (Harrison et al. 1982). Using our group-specific RbcL peptide measurements, we can also calculate taxon-specific potential carbon fixation rates. Notably, the sum of these taxon-specific estimates is below that originating from the broad RbcL peptide (Fig. 2; Table 1).

Discussion

Robust new method for measuring Rubisco concentrations

Our Rubisco measurements captured the major groups in these phytoplankton communities, with minor exceptions: Cryptophytes and Dinoflagellates. Cryptophytes have previously been identified in northern Baffin Bay in early fall, exhibiting a significant negative correlation with nitrogen (Blais et al. 2017), and also in the western Arctic in early spring, before the diatom-dominated spring bloom (Terrado et al. 2011). Though this group was captured by our broad eukaryotic RbcL peptide, additional peptides to quantify their specific contributions to RbcL should be developed. Initially,

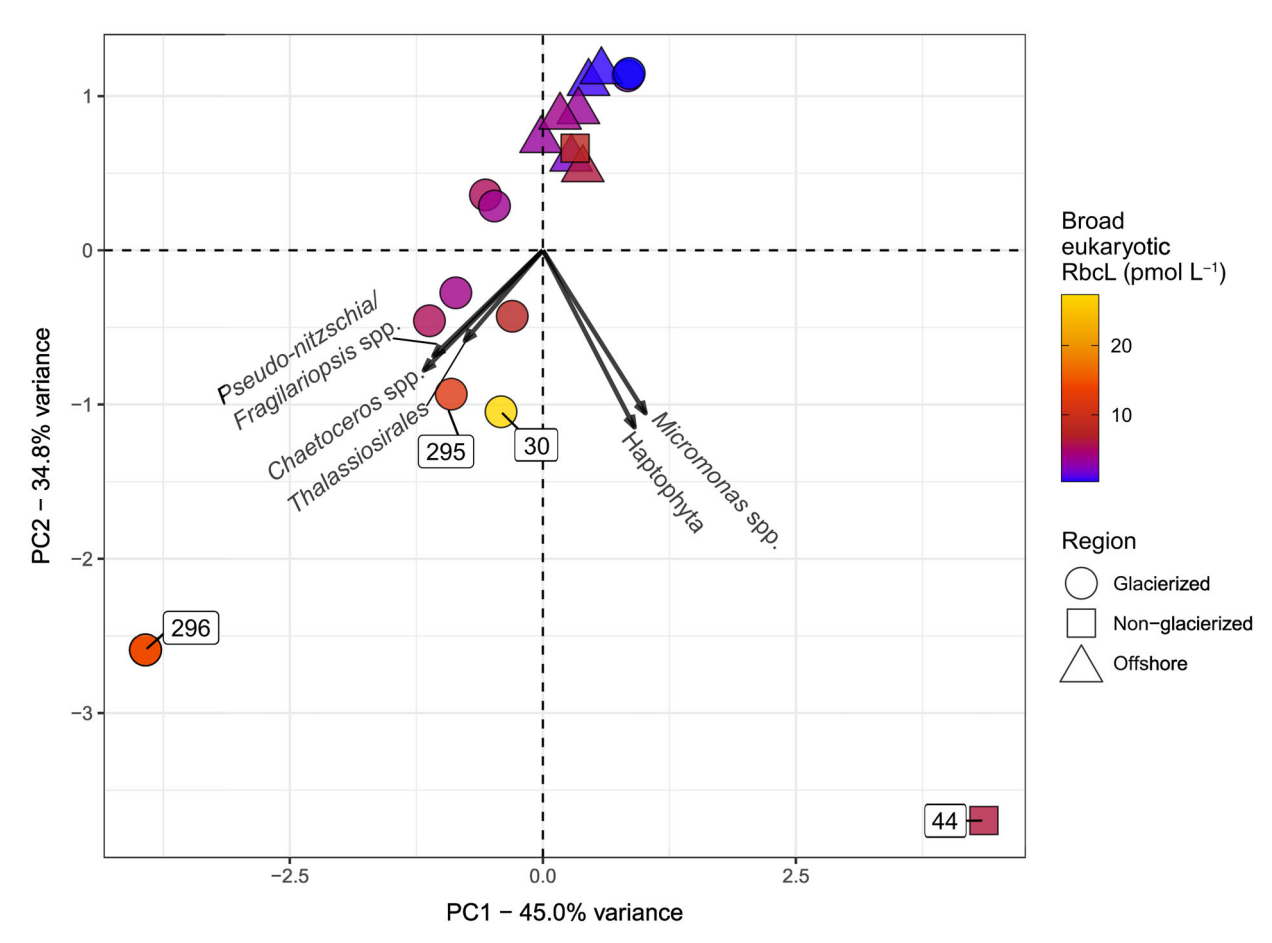


Fig. 6. Principal component analysis of group-specific Rubisco large subunit (RbcL) peptide concentrations from all stations at the subsurface chlorophyll maximum depth, colored by the concentration of the broad RbcL peptide. Points with labels indicate the station that sample is from. Shapes indicate the different regional categories.

we hypothesized that photosynthetic dinoflagellates would make significant contributions to the phytoplankton community in our samples based on previous surveys of the Arctic microbial communities (Lovejoy et al. 2002; Kalenitchenko et al. 2019; Freyria et al. 2021). These studies used 18S rRNA gene

amplicon sequencing which captures both the heterotrophic and photosynthetic microbial community. The chloroplast 16S rRNA sequencing data presented here does not indicate the presence of dinoflagellates, but paired 18S rRNA sequencing data did (Supporting Information Figs. S4, S7). However, 18S

Table 1. Ranges and mean values of primary productivity (PP) across Jones Sound and Baffin Bay taken at the subsurface chlorophyll maximum depth.

Location	Date (month year)	Taxonomic coverage	PP (mg C m ⁻³ d ⁻¹)		
			Range	Average (n)	Reference
Baffin Bay	Sep 1978	Total community	5.7–25.1	13.2 (12)	Harrison et al. (1982) ^a
Jones Sound	Aug/Sep 1983	Total community	0.001-2.02	0.43 (8)	Irwin et al. (1985) ^a
Jones Sound	Aug 2019	Total community	0.01-11.7	1.25 (19)	Present study ^b
Jones Sound	Aug 2019	Diatoms	0–1.55	0.12 (19)	Present study ^b
Jones Sound	Aug 2019	Haptophytes	0.02-1.78	0.16 (19)	Present study ^b
Jones Sound	Aug 2019	Micromonas spp.	0.01–1.13	0.15 (19)	Present study ^b

^aMeasured via ¹⁴C uptake experiments (subject to respiration).

^bMaximum potential carbon fixation rates estimated from RbcL concentrations. Total community rates were estimated using the sum of RbcL from *Micromonas* and the broad RbcL peptide.

rRNA sequecing data is known to over-represent dinoflagellates because of their high 18S rRNA gene copy numbers (Gong and Marchetti 2019). This suggests that either our 16S rRNA gene amplicon analyses are biased against dinoflagellates (Decelle et al. 2015), or that the dinoflagellate species present in this region at the time of sampling relied on heterotrophy and may not be major contributors to Rubisco production. Regardless, dinoflagellates can be important members of Arctic phytoplankton communities, and so developing peptides to quantify their Rubisco is a priority for future work.

The fact that 16S chloroplast rRNA gene sequencing and RbcL peptides resolved relatively similar proportions of targeted groups in each sample is in part surprising, as the abundance of these biomolecules per cell or per unit biomass is expected to vary differently between taxonomic groups (Needham and Fuhrman 2016). We also expected that RbcL concentrations per cell or per unit biomass would change depending on the physiological status of the plankton (e.g., growth phase, nutritional status) (Losh et al. 2013). In contrast, chloroplast 16S rRNA gene copies would be driven largely by number of chloroplasts which can also vary with physiological changes, but to a lesser degree than expected with RbcL concentrations (Needham and Fuhrman 2016). The target group with the most notable proportional difference between these two datasets is Micromonas, suggesting that they may produce a higher ratio of Rubisco to chloroplasts compared to the other phytoplankton groups assessed. This may be expected because *Micromonas* spp. tend to have one chloroplast per cell (Butcher 1952), while diatoms (Hasle and Syvertsen 1997) and *Phaeocystis* (Steidinger and Jangen 1997) can have two or more.

Ecological and biogeochemical insights from RbcL peptides

Given that these RbcL peptide measurements seem to capture the majority of Rubisco produced in these ecosystems, we can further leverage them to gain ecological and biogeochemical insights. Diatoms are classically considered to be important for carbon export as well as quality food for higher trophic levels in marine food webs (Smetacek 1999). For this reason, we are particularly interested in whether nutrient additions at the termini of tidewater glaciers promote the presence of diatom-dominated communities during summer months in Jones Sound. Chaetoceros spp., which we determined to supply higher RbcL concentrations in glacierized regions, have been reported to be the dominant diatom group across the Arctic during bloom periods (Booth et al. 2002; Kalenitchenko et al. 2019; Freyria et al. 2021) and also been reported to persist between bloom periods, when nutrient concentrations are depleted (Schiffrine et al. 2020). Thus, the ubiquity of this species during both bloom and between periods could have important implications for carbon export throughout the year. Although we see higher concentrations of Chaetoceros RbcL at stations classified as glacierized, RbcL concentrations from this group are present across virtually all stations sampled in this study. *Thalassiosira* spp. include larger diatoms that are usually present at the onset of spring blooms in the region, but whose populations decline once nutrient concentrations begin to fall (Lovejoy et al. 2002; Tremblay et al. 2006; Freyria et al. 2021). This pattern of greater *Thalassiosira* spp. abundance under replete nutrient conditions is consistent with our finding of higher RbcL concentrations from *Thalassiosira* spp. near tidewater glaciers in Jones Sound, which can supply nutrients to the surface ocean throughout the summer (Bhatia et al. 2021).

Micromonas spp. have been identified as an important and ubiquitous picophytoplankton group across the Arctic (Joli et al. 2017). These small cells can often dominate the phytoplankton community in the region (Lovejoy et al. 2007) and the dominant strain, Micromonas polaris, has adapted to low temperatures and light in order to thrive in polar conditions throughout the year (Liefer et al. 2019). Generally, smaller phytoplankton, like Micromonas, are able to thrive in low-nutrient conditions and play important roles in nutrient cycling and the microbial loop (Fenchel 2008). The presence of Micromonas in more stratified, nutrient-depleted environments devoid of glaciers is consistent with this role. Though our dataset is limited, it suggests that Micromonas could become increasingly important in coastal regions as tidewater submarine discharge and its associated nutrient delivery to surface water declines in the future. However, though smaller phytoplankton species, like Micromonas, have not traditionally been considered major players in carbon export from the surface ocean, new evidence shows this could change when Micromonas makes up the majority of the phytoplankton community (Bachy et al. 2022). Data from Fram Strait reveals Micromonas spp. comprising up to $\sim 10\%$ of all chloroplast amplicon sequences in sediment traps measured below a Micromonas-dominated phytoplankton community (Bachy et al. 2022).

Phaeocystis spp. can be small free-living cells or form colonies when in bloom conditions (Lancelot et al. 1994). When present in smaller numbers, this phytoplankton group is most likely contributing to recycling-driven production, but when conditions are right for Phaeocystis to form larger colonies, it also has the potential to contribute to carbon export (Verity et al. 2007). A recent study north of Svalbard showed that Phaeocystis-dominated communities supported high amounts of export, nearly as much as those dominated by diatoms (Dybwad et al. 2021). Our results suggest that during the time period sampled in Jones Sound, Phaeocystis generally contributed small amounts of production, but it may have the potential to contribute to export events in the region under different conditions.

We do not expect that the RbcL we occasionally observed well below the euphotic zone (Supporting Information Fig. S5a–d) was produced in situ at that depth, but rather could be present as a result of sinking events. Previous work has reported the utility of Rubisco measurements to examine carbon export to the deep ocean (Orellana and Hansell 2012)

and measure Rubisco at depth in the form of a polymer microgel which falls along the continuum of dissolved and particulate organic material. Rubisco in microgel form was found in concentrations up to $\sim 20~\rm ng~mL^{-1}$ at depths of 2000 m and deeper in the North Pacific. This polymer microgel form seems to protect proteins from biodegradation and enables detection in the deep ocean, allowing the tracking of carbon export from phytoplankton. Efforts by Nunn et al. (2010) measured the degradation of particulate RbcL in a simulated bloom followed by microbial degradation. Particulate RbcL was found to degrade fairly quickly, with no detection of RbcL by Day 10. Future efforts should examine the relationship between particulate and microgel Rubisco concentrations during export events to further explore the utility of deep RbcL measurements to track carbon export.

Rubisco as a fraction of total protein

Calculating Rubisco as a percentage of total protein is of interest because it allows us to compare these data to previous studies, and because it has the potential to provide some insight into the trophic and physiological status of the plankton community. Previous studies have suggested that temperature is the primary driver of what percentage of total protein is made up of Rubisco in pure cultures and in phytoplanktondominated field samples (Losh et al. 2013; Young et al. 2015b, 2016). Nutrient starvation also appears to influence the percentage of protein comprised by Rubisco, but the magnitude of this impact appears to be small compared to temperature (Losh et al. 2013). Field observations of the Rubisco fraction of total protein in Southern Ocean plankton samples and cultures of polar diatom Fragilariopsis cylindrus are relatively high, between 10% and 20%, which is attributed to particularly poor temperature adaptation (Young et al. 2015a,b). In contrast, cultures grown at 20°C under nutrient-replete conditions revealed relatively low Rubisco as a percent of total protein, from 1.4% to 3.7% across eight species of phytoplankton including diatoms, haptophytes, and green algae. An environmental community off the Southern California coast exhibited even lower Rubisco fractions (0.3-2.5%) when incubated at the in situ temperature of 16°C (Losh et al. 2013). Perhaps surprisingly, the calculated percentage range of Rubisco in total protein from our data, collected in an Arctic region with water temperatures hovering around 0°C, is 0.19%-2.0%, which aligns better with low values from mesophilic cultures and environmental data than the psychrophilic diatom cultures and Southern Ocean environmental samples. The Rubisco percentages of total protein we measured in Jones Sound could be driven lower by higher contributions of heterotrophic microbial biomass compared to the intense phytoplankton bloom conditions examined in the Southern Ocean by Young et al. (2015a,b). Similarly, recent studies of a specific Arctic Chaetoceros species, Chaetoceros gelidus, show evidence of the widespread diatom species exhibiting growth rates more similar to temperate phytoplankton species (Schiffrine et al. 2022). It is also important to note that all previous data used to calculate % Rubisco were generated using western blots rather than quantitative mass spectrometry. Peptidebased determinations of % Rubisco in the polar diatom *F. cylindrus*, made using the approach described here, found these values to be between 3% and 8% (Albury 2022). This range is lower than that reported by Young et al. (2015*a*,*b*) and is more consistent with our field data. Future work should continue to examine any systematic differences in these approaches to measuring Rubisco content.

Toward estimating carbon fixation rates

Rubisco is a very inefficient enzyme with low turnover rates, especially at low temperatures (Devos et al. 1998). As such, it has been suggested to be the rate limiting step in the Calvin cycle if light is plentiful and not limiting ATP production (MacIntyre and Geider 1996; Badger et al. 1998). In the Arctic summer, since light is plentiful but temperature remains low, we suggest that Rubisco concentrations would generally reflect carbon fixation rates. However, lower in the water column and in locations where light penetration can be restricted by sediment delivery from glaciers, light limitation could play a role and potentially decouple primary production rates from Rubisco concentrations if cells do not reduce the amount of Rubisco they produce when faced with low light availability. Given this uncertainty, as well as the fact that we have not yet demonstrated a direct relationship between carbon fixation rates and our Rubisco measurements, and that we must rely on a limited set of Rubisco maximum turnover rate measurements to make these estimates (Supporting Information Fig. S3), we conservatively consider our measurements to be a reflection of total and phytoplankton group-specific potential carbon fixation rates. There are currently no techniques available to directly measure the contribution of different plankton groups to primary production. Our peptide-based approach presents a path toward such measurements. However, the sum of our group-specific potential carbon fixation rates currently falls below our estimated total potential production rates. Given that we expect that our group-specific peptides generally cover the most important groups of primary producers in this region (aside from Cryptophytes which appear to only be sporadically important), we suspect that this underestimation may be a result of the presence of some diatom, haptophyte, or green algal species that do not encode our group-specific peptides and hence are not included in these group-specific estimates. Future efforts to obtain additional RbcL sequence information from this environment should be prioritized.

It is evident that there is room for improvement in the selection of RbcL peptides to fully resolve all the major phytoplankton groups present at our stations. Published methodology for measuring RbcL concentrations with Western Blots use RbcL global antibodies designed against peptide tags which are conserved across all known photosynthesizers (Campbell et al. 2003). In contrast, our tryptic peptide-based

approach, via targeted mass spectrometry, requires a suite of measurements, rather than one, to be inclusive of the phytoplankton community as a whole. This has its advantages; in that it allows us to obtain phytoplankton group-specific resolution with our measurements. However, this also means that these peptides need to be continually re-evaluated as we learn more about the dynamic composition of phytoplankton communities and gain access to additional RbcL sequences through both environmental and cultivation-based sequencing approaches.

Conclusions

This targeted metaproteomic approach to quantitatively assess phytoplankton group-specific potential carbon fixation rates is of significant utility for continued monitoring of the dynamic seascape in Jones Sound as glaciers in the region retreat due to climate change. Notably, this approach is amenable to community-based monitoring activities because it requires simple biomass filtration without the need for resource-intensive incubations. If adapted and applied to other marine regions, the tool presented here for assessing carbon fixation potential across phytoplankton groups presents exciting opportunities to quantify phytoplankton group contributions to marine primary productivity and the physiological basis of those contributions using easily acquired and preserved samples.

Data availability statement

Sequenced 16S and 18S rRNA gene data can be accessed at NCBI using Bioproject ID PRJNA905107. CCGS Amundsen oceanographic CTD data are available online at Polar Data Catalog (CCIN reference no. 12713) (Amundsen Science Data Collection, 2019) S/Y Vagabond oceanographic data used in this study are available online at Polar Data Catalog (CCIN reference no. 13211).

References

- Albury, C. 2022. The molecular consequences of vitamin B₁₂ deprivation in the polar diatom, Fragilariopsis cylindrus. Dalhousie University. http://hdl.handle.net/10222/81567
- Apollonio, S. 1973. Glaciers and nutrients in Arctic seas. Science **180**: 491–493.
- Amundsen Science Data Collection. 2019. CTD data collected by the CCGS Amundsen in the Canadian Arctic. ArcticNet Inc., Quebec, Canada. Processed data. Version 1. Archived at www.polardata.ca, Canadian Cryospheric Information Network (CCIN), Waterloo, Canada. doi:10.5884/12713. Accessed on July 2020.
- Audlaluk, L. 2020. What I remember, what I know: The life of a high Arctic exile. Inhabit Media.
- Bachy, C., L. Sudek, C. J. Choi, C. A. Eckmann, E.-M. Nöthig, K. Metfies, and A. Z. Worden. 2022. Phytoplankton surveys in the Arctic Fram Strait demonstrate the tiny eukaryotic

- alga micromonas and other Picoprasinophytes contribute to deep sea export. Microorganisms **10**: 961. doi:10.3390/microorganisms10050961
- Badger, M. R., T. J. Andrews, S. M. Whitney, M. Ludwig, D. C. Yellowlees, W. Leggat, and G. D. Price. 1998. The diversity and coevolution of rubisco, plastids, pyrenoids, and chloroplast-based CO₂-concentrating mechanisms in algae. Can. J. Bot. **76**: 1052–1071. doi:10.1139/b98-074
- Baker, T. S., D. Eisenberg, F. A. Eiserling, and L. Weissman. 1975. The structure of form I crystals of d-ribulose-1,-5-diphosphate carboxylase. J. Mol. Biol. **91**: 391–399. doi: 10.1016/0022-2836(75)90267-3
- Banse, K. 2004. Should we continue to use the 1% light depth convention for estimating the compensation depth of phytoplankton for another 70 years? Limnol. Oceanogr. Bull. **13**: 49–52. doi:10.1002/lob.200413349
- Bhatia, M. P., S. Waterman, D. O. Burgess, P. L. Williams, R. M. Bundy, T. Mellett, M. Roberts, and E. M. Bertrand. 2021. Glaciers and nutrients in the Canadian Arctic archipelago marine system. Global Biogeochem. Cycles **35**: e2021GB006976. doi:10.1029/2021GB006976
- Blais, M., and others. 2017. Contrasting interannual changes in phytoplankton productivity and community structure in the coastal Canadian Arctic Ocean. Limnol. Oceanogr. **62**: 2480–2497. doi:10.1002/lno.10581
- Booth, B. C., P. Larouche, S. Bélanger, B. Klein, D. Amiel, and Z.-P. Mei. 2002. Dynamics of Chaetoceros socialis blooms in the north water. Deep Sea Res. II Top. Stud. Oceanogr. **49**: 5003–5025. doi:10.1016/S0967-0645(02)00175-3
- Butcher, R. 1952. Contributions to our knowledge of the smaller marine algae. J. Mar. Biol. Assoc. UK. **31**: 175–191.
- Campbell, D. A., A. M. Cockshutt, and J. Porankiewicz-Asplund. 2003. Analysing photosynthetic complexes in uncharacterized species or mixed microalgal communities using global antibodies. Physiol. Plant. **119**: 322–327. doi: 10.1034/j.1399-3054.2003.00175.x
- Comeau, A. M., W. K. W. Li, J.-É. Tremblay, E. C. Carmack, and C. Lovejoy. 2011. Arctic Ocean microbial community structure before and after the 2007 Record Sea ice minimum. PloS One **6**: e27492. doi:10.1371/journal.pone. 0027492
- Decelle, J., and others. 2015. PhytoREF: A reference database of the plastidial 16S rRNA gene of photosynthetic eukaryotes with curated taxonomy. Mol. Ecol. Resour. **15**: 1435–1445. doi:10.1111/1755-0998.12401
- Devos, N., M. Ingouff, R. Loppes, and R. F. Matagne. 1998. Rubisco adaptation to low temperatures: A comparative study in psychrophilic and mesophilic unicellular algae. J. Phycol. **34**: 655–660. doi:10.1046/j.1529-8817.1998. 340655.x
- Dunse, T., K. Dong, K. S. Aas, and L. C. Stige. 2022. Regional-scale phytoplankton dynamics and their association with glacier meltwater runoff in Svalbard. Biogeosciences **19**: 271–294. doi:10.5194/bg-19-271-2022

- Dybwad, C., and others. 2021. Carbon export in the Seasonal Sea ice zone north of Svalbard from winter to late summer. Front. Mar. Sci. 7.
- Fenchel, T. 2008. The microbial loop—25 years later. J. Exp. Mar. Biol. Ecol. **366**: 99–103. doi:10.1016/j.jembe.2008. 07.013
- Freyria, N. J., N. Joli, and C. Lovejoy. 2021. A decadal perspective on north water microbial eukaryotes as Arctic Ocean sentinels. Sci. Rep. **11**: 8413. doi:10.1038/s41598-021-87906-4
- Gasteiger, E., C. Hoogland, A. Gattiker, S. Duvaud, M. R. Wilkins, R. D. Appel, and A. Bairoch. 2005. Protein identification and analysis tools on the ExPASy server, p. 571–607. *In* J. M. Walker [ed.], The proteomics protocols handbook. Humana Press.
- Gong, W., and A. Marchetti. 2019. Estimation of 18S gene copy number in marine eukaryotic plankton using a next-generation sequencing approach. Front. Mar. Sci. 6.
- Gurdeep Singh, R., and others. 2019. Unipept 4.0: Functional analysis of metaproteome data. J. Proteome Res. **18**: 606–615. doi:10.1021/acs.jproteome.8b00716
- Hansen, H. P., and F. Koroleff. 1999. Determination of nutrients, p. 159–228. *In* K. Grasshoff, K. Kremling, and M. Ehrhardt [eds.], Methods of seawater analysis. Wiley-VCH.
- Harrison, W. G., T. Platt, and B. Irwin. 1982. Primary production and nutrient assimilation by natural phytoplankton populations of the eastern Canadian Arctic. Can. J. Fish. Aquat. Sci. **39**: 335–345. doi:10.1139/f82-046
- Harrison, W. G., W. K. W. Li, J. C. Smith, E. J. H. Head, and A. R. Longhurst. 1987. Depth profiles of plankton, particulate organic matter and microbial activity in the eastern Canadian Arctic during summer. Polar Biol. **7**: 207–224. doi:10.1007/BF00287417
- Hartman, F. C., and M. R. Harpel. 1994. Structure, function, regulation, and assembly of p-ribulose-1,5-bisphosphate carboxylase/oxygenase. Annu. Rev. Biochem. **63**: 197–232. doi:10.1146/annurev.bi.63.070194.001213
- Hasle, G. R., and E. E. Syvertsen. 1997. Chapter 2—Marine diatoms, p. 5–385. *In* C. R. Tomas [ed.], Identifying marine phytoplankton. Academic Press.
- Hopwood, M. J., and others. 2020. Review article: How does glacier discharge affect marine biogeochemistry and primary production in the Arctic? Cryosphere **14**: 1347–1383. doi:10.5194/tc-14-1347-2020
- Irwin, B., T. Platt, and C. Caverhill. 1985. Primary production and other related measurements in the eastern Canadian arctic during summer of 1983. Canadian data report of fisheries and aquatic sciences; No. 510.
- John, D. E., S. S. Patterson, and J. H. Paul. 2007. Phytoplank-ton-group specific quantitative polymerase chain reaction assays for RuBisCO mRNA transcripts in seawater. Marine Biotechnol. 9: 747–759. doi:10.1007/s10126-007-9027-z
- Joli, N., A. Monier, R. Logares, and C. Lovejoy. 2017. Seasonal patterns in Arctic prasinophytes and inferred ecology of

- Bathycoccus unveiled in an Arctic winter metagenome. ISME J. **11**: 1372–1385. doi:10.1038/ismej.2017.7
- Joli, N., M. Gosselin, M. Ardyna, M. Babin, D. F. Onda, J.-É. Tremblay, and C. Lovejoy. 2018. Need for focus on microbial species following ice melt and changing freshwater regimes in a Janus Arctic Gateway. Sci. Rep. 8: 1–11. doi:10. 1038/s41598-018-27705-6
- Jones, E. P., J. H. Swift, L. G. Anderson, M. Lipizer, G. Civitarese, K. K. Falkner, G. Kattner, and F. McLaughlin. 2003. Tracing Pacific water in the North Atlantic Ocean. J. Geophys. Res. Oceans 108: 3116. doi:10.1029/2001JC001141
- Joy-Warren, H. L., and others. 2022. Springtime phytoplankton responses to light and iron availability along the western Antarctic Peninsula. Limnol. Oceanogr. **67**: 800–815. doi:10.1002/lno.12035
- Kalenitchenko, D., N. Joli, M. Potvin, J.-É. Tremblay, and C. Lovejoy. 2019. Biodiversity and species change in the Arctic Ocean: A view through the lens of Nares Strait. Front. Mar. Sci. Lausanne. **6.** doi:10.3389/fmars.2019.00479
- Kanna, N., and others. 2022. Meltwater discharge from marine-terminating glaciers drives biogeochemical conditions in a Greenlandic fjord. Glob. Biogeochem. Cycles **36**: e2022GB007411. doi:10.1029/2022GB007411
- Lancelot, C., P. Wassmann, and H. Barth. 1994. Ecology of Phaeocystis-dominated ecosystems. J. Mar. Syst. **5**: 1–4. doi: 10.1016/0924-7963(94)90012-4
- Liefer, J. D., and others. 2019. The macromolecular basis of phytoplankton C:N:P under nitrogen starvation. Front. Microbiol. **10**. doi:10.3389/fmicb.2019.00763
- Lorimer, G. H., and T. J. Andrews. 1973. Plant photorespiration—An inevitable consequence of the existence of atmospheric oxygen. Nature **243**: 359–360. doi:10. 1038/243359a0
- Losh, J. L., J. N. Young, and F. M. M. Morel. 2013. Rubisco is a small fraction of total protein in marine phytoplankton. New Phytol. **198**: 52–58. doi:10.1111/nph.12143
- Lovejoy, C. 2014. Changing views of Arctic protists (marine microbial eukaryotes) in a changing Arctic. Acta Protozool. **53**: 91–100. doi:10.4467/16890027AP.14.009.1
- Lovejoy, C., L. Legendre, M.-J. Martineau, J. Bâcle, and C. H. von Quillfeldt. 2002. Distribution of phytoplankton and other protists in the North Water. Deep Sea Res. II Top. Stud. Oceanogr. **49**: 5027–5047. doi:10.1016/S0967-0645 (02)00176-5
- Lovejoy, C., and others. 2007. Distribution, phylogeny, and growth of cold-adapted picoprasinophytes in Arctic Seas1. J. Phycol. **43**: 78–89. doi:10.1111/j.1529-8817.2006.00310.x
- MacIntyre, H. L., and R. J. Geider. 1996. Regulation of Rubisco activity and its potential effect on photosynthesis during mixing in a turbid estuary. Mar. Ecol. Prog. Ser. **144**: 247–264.
- Madeira, F., and others. 2022. Search and sequence analysis tools services from EMBL-EBI in 2022. Nucleic Acids Res. **50**: W276–W279. doi:10.1093/nar/gkac240

- Maselli, M., L. Meire, P. Meire, and P. J. Hansen. 2023. Effects of glacial flour on marine micro-plankton: Evidences from natural communities of Greenlandic fjords and experimental studies. Protist **174**: 125928. doi:10.1016/j.protis.2022. 125928
- McGrath, T., M. Cronin, E. Kerrigan, D. Wallace, C. Gregory, C. Normandeau, and E. McGovern. 2019. A rare intercomparison of nutrient analysis at sea: Lessons learned and recommendations to enhance comparability of openocean nutrient data. Earth Syst. Sci. Data 11: 355–374. doi: 10.5194/essd-11-355-2019
- Meire, L., and others. 2017. Marine-terminating glaciers sustain high productivity in Greenland fjords. Global Change Biol. **23**: 5344–5357. doi:10.1111/gcb.13801
- Miller, C. B., and P. A. Wheeler. 2012. Biological oceanography. Wiley.
- Monier, A., J. Comte, M. Babin, A. Forest, A. Matsuoka, and C. Lovejoy. 2015. Oceanographic structure drives the assembly processes of microbial eukaryotic communities. ISME J. **9**: 990–1002. doi:10.1038/ismej.2014.197
- Morse, D., P. Salois, P. Markovic, and J. W. Hastings. 1995. A nuclear-encoded form II RuBisCO in dinoflagellates. Science 268: 1622–1624.
- Murray, C., S. Markager, C. A. Stedmon, T. Juul-Pedersen, M. K. Sejr, and A. Bruhn. 2015. The influence of glacial melt water on bio-optical properties in two contrasting Greenlandic fjords. Estuar. Coast. Shelf Sci. **163**: 72–83. doi:10.1016/j.ecss.2015.05.041
- Needham, D. M., and J. A. Fuhrman. 2016. Pronounced daily succession of phytoplankton, archaea and bacteria following a spring bloom. Nat. Microbiol. 1: 1–7. doi:10.1038/nmicrobiol.2016.5
- Nunn, B. L., Y. S. Ting, L. Malmström, Y. S. Tsai, A. Squier, D. R. Goodlett, and H. R. Harvey. 2010. The path to preservation: Using proteomics to decipher the fate of diatom proteins during microbial degradation. Limnol. Oceanogr. 55: 1790–1804. doi:10.4319/lo.2010.55.4.1790
- Orellana, M. N. V., and D. A. Hansell. 2012. Ribulose-1,-5-bisphosphate carboxylase/oxygenase (RuBisCO): A long-lived protein in the deep ocean. Limnol. Oceanogr. **57**: 826–834. doi:10.4319/lo.2012.57.3.0826
- Parada, A. E., D. M. Needham, and J. A. Fuhrman. 2016. Every base matters: Assessing small subunit rRNA primers for marine microbiomes with mock communities, time series and global field samples. Environ. Microbiol. **18**: 1403–1414. doi:10.1111/1462-2920.13023
- Pino, L. K., B. C. Searle, J. G. Bollinger, B. Nunn, B. MacLean, and M. J. MacCoss. 2017. The skyline ecosystem: Informatics for quantitative mass spectrometry proteomics. Mass Spectrom. Rev. **39**: 229–244. doi:10.1002/mas.21540
- Pujari, L., and others. 2019. Diversity and spatial distribution of Chromophytic phytoplankton in the Bay of Bengal revealed by RuBisCO genes (rbcL). Front. Microbiol. **10**. doi: 10.3389/fmicb.2019.01501

- Quince, C., A. Lanzen, R. J. Davenport, and P. J. Turnbaugh. 2011. Removing noise from pyrosequenced amplicons. BMC Bioinformatics **12**: 38. doi:10.1186/1471-2105-12-38
- Schiffrine, N., J.-É. Tremblay, and M. Babin. 2020. Growth and elemental stoichiometry of the ecologically-relevant Arctic diatom *Chaetoceros gelidus*: A mix of polar and temperate. Front. Mar. Sci. 6.
- Schiffrine, N., J.-É. Tremblay, and M. Babin. 2022. Interactive effects of temperature and nitrogen source on the elemental stoichiometry of a polar diatom. Limnol. Oceanogr. **67**: 2750–2762. doi:10.1002/lno.12235
- Smetacek, V. 1999. Diatoms and the ocean carbon cycle. Protist **150**: 25–32. doi:10.1016/S1434-4610(99)70006-4
- Steidinger, K. A., and K. Jangen. 1997. Chapter 3—Dinoflagellates, p. 387–584. *In* C. R. Tomas [ed.], Identifying marine phytoplankton. Academic Press.
- Tabita, F. R., T. E. Hanson, H. Li, S. Satagopan, J. Singh, and S. Chan. 2007. Function, structure, and evolution of the RubisCO-like proteins and their RubisCO homologs. Microbiol. Mol. Biol. Rev. 71: 576–599. doi:10.1128/MMBR.00015-07
- Tabita, F. R., T. E. Hanson, S. Satagopan, B. H. Witte, and N. E. Kreel. 2008. Phylogenetic and evolutionary relationships of RubisCO and the RubisCO-like proteins and the functional lessons provided by diverse molecular forms. Philos. Trans. R. Soc. B Biol. Sci. **363**: 2629–2640. doi:10.1098/rstb.2008. 0023
- Terrado, R., E. Medrinal, C. Dasilva, M. Thaler, W. F. Vincent, and C. Lovejoy. 2011. Protist community composition during spring in an Arctic flaw lead polynya. Polar Biol. **34**: 1901–1914. doi:10.1007/s00300-011-1039-5
- Tremblay, J.-É., C. Michel, K. A. Hobson, M. Gosselin, and N. M. Price. 2006. Bloom dynamics in early opening waters of the Arctic Ocean. Limnol. Oceanogr. **51**: 900–912. doi: 10.4319/lo.2006.51.2.0900
- Tremblay, J.-É., L. G. Anderson, P. Matrai, P. Coupel, S. Bélanger, C. Michel, and M. Reigstad. 2015. Global and regional drivers of nutrient supply, primary production and CO₂ drawdown in the changing Arctic Ocean. Prog. Oceanogr. **139**: 171–196. doi:10.1016/j.pocean.2015. 08.009
- Verity, P. G., C. P. Brussaard, J. C. Nejstgaard, M. A. van Leeuwe, C. Lancelot, and L. K. Medlin. 2007. Current understanding of Phaeocystis ecology and biogeochemistry, and perspectives for future research. Biogeochemistry **83**: 311–330. doi:10.1007/s10533-007-9090-6
- Vonnahme, T. R., E. Persson, U. Dietrich, E. Hejdukova, C. Dybwad, J. Elster, M. Chierici, and R. Gradinger. 2021.
 Early spring subglacial discharge plumes fuel under-ice primary production at a Svalbard tidewater glacier. Cryosphere
 15: 2083–2107. doi:10.5194/tc-15-2083-2021
- Wu, M., J. S. P. McCain, E. Rowland, R. Middag, M. Sandgren,A. E. Allen, and E. M. Bertrand. 2019. Manganese and iron deficiency in Southern Ocean *Phaeocystis antarctica*

Roberts et al. Rubisco in glacier-marine systems

populations revealed through taxon-specific protein indicators. Nat. Commun. **10**: 3582. doi:10.1038/s41467-019-11426-z

Young, J. N., J. A. L. Goldman, S. A. Kranz, P. D. Tortell, and F. M. M. Morel. 2015a. Slow carboxylation of Rubisco constrains the rate of carbon fixation during Antarctic phytoplankton blooms. New Phytol. 205: 172–181. doi:10.1111/ nph.13021

Young, J. N., S. A. Kranz, J. A. L. Goldman, P. D. Tortell, and F. M. M. Morel. 2015*b*. Antarctic phytoplankton downregulate their carbon-concentrating mechanisms under high CO₂ with no change in growth rates. Mar. Ecol. Prog. Ser. **532**: 13–28. doi:10.3354/meps11336

Young, J. N., A. M. C. Heureux, R. E. Sharwood, R. E. M. Rickaby, F. M. M. Morel, and S. M. Whitney. 2016. Large variation in the Rubisco kinetics of diatoms reveals diversity among their carbon-concentrating mechanisms. J. Exp. Bot. **67**: 3445–3456. doi:10.1093/jxb/erw163

Acknowledgments

We thank David Burgess (Natural Resources Canada) for invaluable assistance in research program building and in water column sampling aboard the *S/Y Vagabond*. We thank Jimmy Qaapik, the Hamlet of Grise Fiord, the Brossier Family and *S/Y Vagabond*, Andrew Hamilton, the Polar Continental Shelf Program (PCSP) as well as Pascale Guillot (Québec-Océan) and the rest

of the CCGS Amundsen crew and Amundsen Science team for their invaluable assistance in the field and at sea. Some of the data presented herein were collected by the Canadian research icebreaker CCGS Amundsen and made available by the Amundsen Science program, which was supported by the Canada Foundation for Innovation and Natural Sciences and Engineering Research Council of Canada. The views expressed in this publication do not necessarily represent the views of Amundsen Science or that of its partners. We also thank Liz Kerrigan for nutrient analyses, and Gianpaolo Cardellini for Rubisco database building assistance. We are grateful to Connie Loveiov, Diana Varela, Emmanuel Devred, and Zoe Finkel for illuminating discussions and critical feedback. Funding for this work was provided by NSERC Discovery Grant RGPIN-2015-05009 to E.M.B., Canada Research Chairs to S.W. and E.M.B., a Simons Foundation award 504183 to E.M.B., New Frontiers in Research Fund exploration award NFRFE-2018-01-427 to E.M.B., S.W., M.P.B., and I. Oaapik, NSERC Shiptime grant RGPST-544982-2020, PCSP grant 68719 to M.P.B., Simons Foundation Award 561645, Sloan Fellowship, and NSF Polar Programs OP 17445 to J.N.Y., and ArcticNet (a Network of Centres of Excellence Canada).

Conflict of Interest

The authors declare no conflicts of interest.

Submitted 27 January 2023 Revised 22 January 2024 Accepted 23 January 2024

Associate editor: Tatiana Rynearson